ISSN 1070-3284, Russian Journal of Coordination Chemistry, 2022, Vol. 48, No. 3, pp. 153–163. © Pleiades Publishing, Ltd., 2022.
Russian Text © The Author(s), 2022, published in Koordinatsionnaya Khimiya, 2022, Vol. 48, No. 3, pp. 157–167.

Dedicated to the memory of Academician Ilya Iosifovich Moiseev

Synthesis and Structure of Heterometallic Palladium and Iron Complexes

I. A. Yakushev[a, *, **], **M. A. Dyuzheva**[a, b], **I. A. Stebletsova**[b], **A. B. Kornev**[a], **N. V. Cherkashina**[a], **and M. N. Vargaftik**[a]

[a] *Kurnakov Institute of General and Inorganic Chemistry, Russian Academy of Sciences, Moscow, 119991 Russia*
[b] *Higher Chemical College, Russian Academy of Sciences, Mendeleev University of Chemical Technology of Russia, Moscow, 125047 Russia*
**e-mail: ilya.yakushev@igic.ras.ru*
***e-mail: cs68@mail.ru*

Received May 12, 2021; revised September 09, 2021; accepted September 13, 2021

Abstract—Heterometallic palladium(II) complexes with ferrocenecarboxylic acid FcCOOH were synthesized and structurally characterized for the first time. The reactions of mononuclear $[Pd(Py)_2(OOCMe)_2]$ and $[Pd(Phen)(OOCMe)_2]$ complexes with FcCOOH were accompanied by easy displacement of acetate anions from the inner sphere by the ferrocenecarboxylate anions to give iron-containing molecular palladium complexes: three solvatomorphs of $[Pd(Py)_2(FcCOO)_2]$ with benzene (**I**, **II**) and dichloromethane (**III**); the use of $[Pd(Phen)(OOCMe)_2]$ as the starting compound resulted in the formation of the heteroligand acetate ferrocenecarboxylate $[Pd(Phen)(FcCOO)_2Pd(Phen)(FcCOO)(OOCMe)]$ (**IV**). Fully substituted $[Pd(Phen)(FcCOO)_2]$ (**V**) was prepared by successive treatment of palladium acetate $[Pd_3(OOCMe)_6]$ with FcCOOH and 1,10-phenanthroline. The structures of complexes **I**–**V** were studied by X-ray diffraction (CIF files CCDC nos. 2078399–2078403).

Key words: palladium, acetate complexes, ferrocenecarboxylic acid, synthesis, X-ray diffraction, crystal chemistry

DOI: 10.1134/S107032842203006X

INTRODUCTION

A relevant task of modern chemistry is to develop methods for the synthesis of high-performance catalysts for industrially important catalytic processes such as hydrocarbon cracking and reforming in petrochemistry, production of motor fuels and lubrication materials from renewable sources, purification of monomers from impurities, and development of homogeneous and heterogeneous catalysts for pharmaceutical industry and fine organic synthesis. Switching from monometallic to bi- and polymetallic catalysts both for homogeneous catalysis [1] and for the preparation of supported heterogeneous catalysts [2] often increases the selectivity of the catalyzed reaction and the catalyst activity, extends the catalyst service life, and improves the performance characteristics.

One method for preparing supported mixed catalysts includes the use of bi- and polymetallic complexes as the precursors of nanoalloys [2–6] and mixed-metal nanoparticles [7]; it is important that these precursors do not contain phosphorus, chlorine, sulfur, and other components that are difficult to remove.

Previously, it was shown that heterometallic palladium acetate and pivalate complexes $[Pd^{II}(OOCR)_4M^{II}]$ can be synthesized from readily available palladium acetate and acetates of extra metals M [8–12]; some of the compounds showed high catalytic activity and selectivity in the homogeneous hydrogenation of unsaturated hydrocarbons [13] and in C–H-bond aziridination and amination [14], as precursors of catalysts for selective hydrogenation of alkyne triple bonds [15–19], and as efficient catalysts for oxygen reduction [20].

Mixed carboxylate complexes of this type were also obtained for platinum [21], in particular platinum(II) acetate and pivalate complexes with iron(III) [22, 23]; however, attempts to obtain palladium and iron complexes, similar to those for platinum, did not meet with success.

An alternative method for the introduction of a non-noble metal into precursors of catalytically active materials is the use of metal-containing carboxylic acids as ligands; examples are cymantrenecarboxylic acid (which was used to prepare bi- and even trimetallic complexes [24, 25]) and ferrocenecarboxylic acid, which was used previously to obtain mixed-metal complexes with platinum(II) [26]. This paper addresses the use of ferrocenecarboxylic acid for the synthesis of heterometallic palladium(II) compounds (**I**–**V**).

EXPERIMENTAL

The solvents used in the study (dichloromethane, acetone, benzene, pyridine) were purified by standard procedures [27]. 1,10-Phenanthroline (Phen, 99%, Alfa Aesar) and ferrocenecarboxylic acid (FcCOOH, 97%, Sigma-Aldrich) were used as received. Palladium(II) acetate $[Pd_3(OOCMe)_6]$ (high-purity grade, Reakhim) was refluxed in glacial acetic acid with freshly prepared palladium black and recrystallized from acetic acid.

Elemental analysis was carried out on a EuroVector EA3000 automated C,H,N-analyzer (Italy, 2008). Infrared spectra were measured on a Bruker Alpha FTIR spectrometer in the attenuated total reflection (ATR) mode in the 4000–400 cm^{-1} range.

Synthesis of $[Pd(Py)_2(FcCOO)_2]\cdot C_6H_6$ (I) was performed in two steps. The intermediate $[Pd(Py)_2(OOCMe)_2]$ was prepared by modification of a reported procedure [28]: $[Pd_3(OOCMe)_6]$ (117 mg, 0.174 mmol) was dissolved in a mixture of benzene (16 mL) and chloroform (4 mL), the resulting solution was filtered, and pyridine (84 μL, 82 mg, 1.04 mmol) was added, with the solution color being changed to light yellow. A solution of FcCOOH (240 mg, 1.04 mmol) in benzene (5 mL) was added to the resulting solution of the mononuclear complex $[Pd(Py)_2(OOCMe)_2]$, the mixture was magnetically stirred without heating for 30 min and allowed to crystallize with slow evaporation. The resulting yellow crystals were separated from the mother liquor by decantation, washed with a small amount of cold benzene, and dried in an argon flow. The yield of complex **I** was 400 mg (96% based on Pd). The compound readily loses the solvent of crystallization when stored in air.

For $C_{38}H_{34}N_2O_4Fe_2Pd$

Anal. calcd., %	C, 56.99	H, 4.28	N, 3.50
Found, %	C, 56.38	H, 4.15	N, 3.66

IR (ATR; ν, cm^{-1}): 2928 br.w, 1650 w, 1615 s, 1468 w, 1467 m, 1376 w, 1287 m, 1156 m, 1036 w, 1004 w, 798 m, 780 m, 667 s, 480 m, 455 m.

Synthesis of $[Pd(Py)_2(FcCOO)_2]\cdot 3C_6H_6$ (II). Compound **I** (60 mg) was dissolved in warm benzene (75 mL). Slow evaporation of the solvent gave light yellow needle crystals, relatively unstable without the mother liquor. The yield of complex **II** was 64 mg (89%).

For $C_{50}H_{46}N_2O_4Fe_2Pd$

Anal. calcd., %	C, 62.75	H, 4.84	N, 2.93
Found, %	C, 62.31	H, 4.64	N, 2.98

IR (ATR; ν, cm^{-1}): 2923 br.w, 1652 w, 1615 m, 1477 m, 1449 s, 1374 s, 1310 s, 1242 s, 1171 s, 1103 m, 1066 w, 1029 w, 1002 w, 919 w, 802 m, 766 m, 674 s, 483 s, 452 m.

Synthesis of $[Pd(Py)_2(FcCOO)_2]\cdot 2CH_2Cl_2$ (III) was carried out by recrystallization of complex **I** from dichloromethane. Complex **I** readily dissolved in CH_2Cl_2 without heating (50 mg of the complex in 25 mL of CH_2Cl_2), and slow drying of the solution gave crystals of **III**. The yield of complex **III** was 52 mg (93%).

For $C_{34}H_{32}Cl_4N_2O_4Fe_2Pd$

Anal. calcd., %	C, 45.75	H, 3.61	N, 3.14
Found, %	C, 46.88	H, 3.84	N, 3.25

IR (ATR; ν, cm^{-1}): 3375 br.w, 3034 w, 1564 m, 1411 s, 1376 m, 1316 s, 1273 m, 1173 m, 1072 m, 1022 m, 1003 m, 918 w, 788 m, 764 m, 731 m, 691 s, 655 w, 628 m, 581 w, 513 m, 478 s, 445 w.

Synthesis of $[Pd(Phen)(FcCOO)_2Pd(Phen)(FcCOO)(OOCMe)]$ (IV). Weighed portions of $[Pd(Phen)(OOCMe)_2]$ (100 mg, 0.247 mmol) (prepared by previously reported procedure [29]) and FcCOOH (114 mg, 0.495 mmol) were separately dissolved in 20 and 15 mL of methanol, respectively. The solutions were mixed and allowed to stand at room temperature. The orange crystals suitable for X-ray diffraction that formed within 5 days were separated by decantation and washed with a small amount of cold methanol to remove the remaining FcCOOH. The yield of complex **IV** was 78 mg (48% based on Pd).

For $C_{59}H_{46}N_4O_8Fe_3Pd_2$

Anal. calcd., %	C, 53.71	H, 3.51	N, 4.25
Found, %	C, 52.95	H, 3.91	N, 4.03

IR (ATR; ν, cm^{-1}): 3166 br.w, 1703 s, 1608 s, 1379 s, 1331 s, 1249 s, 1022 m, 889 m, 695 s, 622 s, 448 w.

Synthesis of $[Pd(Phen)(FcCOO)_2]$ (V) was carried out in two steps. The first step was treatment of $[Pd_3(OOCMe)_6]$ (100 mg, 0.148 mmol) with a stoichiometric amount of FcCOOH (205 mg, 0.891 mmol) in dichloromethane (120 mL). The resulting red-brown solution was refluxed for 50 min and then re-evaporated three times under reduced pressure with small portions of dichloromethane to remove residual acetic acid. The resulting dark brown product was dried in a vacuum desiccator. As the second step, palladium ferrocenecarboxylate $[Pd(FcCOO)_2]_n$ (100 mg, 0.177 mmol) was dissolved in acetone (10 mL), and a solution of Phen (32 mg, 0.178 mmol) in acetone (5 mL) was added. Prior to mixing, both solutions were filtered to remove traces of particulate matter. The reaction mixture was magnetically stirred for 30 min at room temperature. A week later, single crystals suitable for X-ray diffraction were found on the walls of the flask. An additional portion of the product was obtained upon evaporation of the mother liquor on a rotary evaporator to a minimum volume and subsequent crystallization at low temperature (5°C). The total yield of complex **V** was 122 mg (92% based on Pd).

For $C_{34}H_{26}N_2O_4Fe_2Pd$

Anal. calcd., %	C, 54.84	H, 3.52	N, 3.76
Found, %	C, 55.30	H, 4.02	N, 3.55

IR (ATR, ν, mA^{-1}): 2482 s, 2458 s, 2406 m, 2388 m, 2360 m, 2318 s, 2271 s, 2222 s, 2197 w, 2172 w, 2117 m, 2102 m, 2042 m, 1994 s, 1960 m, 1903 s, 1865 m, 1852 s, 1814 m, 1797 s, 1751 w, 1619 m, 651 m.

X-ray diffraction. The X-ray diffraction data for complexes **I** and **V** were collected on a Bruker D8 Venture Photon diffractometer in φ and ω scan modes at the Center for Collective Use of the Kurnakov Institute of General and Inorganic Chemistry, Russian Academy of Sciences, at 100(2) K (λ = 0.71073 Å, Incoatec IμS 3.0 microfocus X-ray source). The primary initiation, refinement of unit cell parameters, and integration of reflections were performed using the Bruker APEX3 program package [30]. The absorption corrections were applied using the SADABS program package [30].

X-ray diffraction data for complexes **II**–**IV** were obtained on the Belok crystallography beamline of the Kurchatov Synchrotron Radiation Source at the National Research Center "Kurchatov Institute" (Moscow, Russian Federation) in the φ-scan mode using a Rayonix SX165 CCD array detector at 100(2) K (λ = 0.74500 and 0.74539 Å) [31]. The XDS program package was used for primary indexing, refinement of unit cell parameters, and integration of reflections and to apply absorption corrections [32].

The structures of **I**–**V** were solved by direct methods [33] and refined in the anisotropic approximation by full-matrix least-squares method on F^2 for all non-hydrogen atoms [34]. In view of the disorder of one of the cyclopentadienyl groups of ferrocenecarboxylic acid in complex **IV** over two positions (0.52 : 0.48 occupancy ratio), both components were refined with constraints on the geometric parameters and thermal displacements of atoms (AFIX, SIMU, DELU). In the refinement of all structures, hydrogen atoms were placed into calculated positions and refined in the riding model with $U_{iso}(H) = 1.5U_{equiv}(C)$ for methyl hydrogen atoms and $1.2U_{equiv}(C)$ for the hydrogen atoms of benzene, dichloromethane, and aromatic ligands. The residual electron density corresponding to the disordered neutral solvent was removed from the refinement model for structures **IV** and **V** by means of SQUEEZE procedure in the PLATON software [35].

The calculations were carried out using the SHELXTL program package [34] in the OLEX2 structural data visualization and processing medium [36]. The crystallographic data and structure refinement details for structures **I**–**V** are summarized in Table 1.

The structural parameters for compounds **I**–**V** were deposited with the Cambridge Crystallographic Data Centre (CCDC nos. 2078399–2078403; deposit@ccdc.cam.ac.uk or http://www.ccdc.cam.ac.uk/data_request/cif).

RESULTS AND DISCUSSION

The substitution of labile acetate ligands is a popular method for changing the molecular design and for preparing new derivatives of many palladium and platinum carboxylate complexes, in particular heteronuclear ones; for example, the replacement of acetate groups by pivalate groups can be used to increase the solubility of metal complexes in non-polar solvents [11, 23]. Organometallic carboxylic acids, in particular cymantrenecarboxylic acid, are introduced into the carboxylate complexes of noble and non-noble metals similarly to purely organic carboxylic acids [37–39], e.g., for the synthesis of complexes with 2,6-lutidine [40]. Ferrocenecarboxylic acid is an available reagent for the preparation of heterometallic compounds of copper [41] and platinum [26], and other systems of this type.

Palladium acetate $[Pd_3(OOCMe)_6]$ readily reacts with pyridine under mild conditions; this gives mononuclear *trans*-complex $[Pd(Py)_2(OOCMe)_2]$ in an almost quantitative yield. The addition of two equivalents of ferrocenecarboxylic acid FcCOOH in a nonpolar medium to the reaction mixture induces the replacement of acetate anions and formation of crystalline $[Pd(Py)_2(FcCOO)_2]\cdot C_6H_6$ (**I**) (Fig. 1). The light yellow crystals of the complex lose the solvent of crystallization in air, but are easily recrystallized from benzene or dichloromethane to give solvatomorphs $[Pd(Py)_2(FcCOO)_2\cdot 3C_6H_6]$ (**II**) (Fig. 2) and $[Pd(Py)_2(FcCOO)_2]\cdot 2CH_2Cl_2$ (**III**) (Fig. 3), respectively. According to X-ray diffraction data, compounds **I** and **III** crystallize in triclinic space group $P\bar{1}$, unlike solvatomorph **II**, which crystallizes in monoclinic space group $P2_1/c$. In each molecule, the palladium atom is in the square planar environment of two ferrocenecarboxylate oxygen atoms and pyridine

Table 1. Crystallographic data and structure refinement details for complexes **I–V**

Parameter	Value				
	I	**II**	**III**	**IV**	**V**
Molecular formula	$C_{38}H_{34}N_2O_4Fe_2Pd$	$C_{50}H_{46}N_2O_4Fe_2Pd$	$C_{34}H_{32}Cl_4N_2O_4Fe_2Pd$	$C_{59}H_{46}N_4O_8Fe_3Pd_2$	$C_{34}H_{26}N_2O_4Fe_2Pd$
M	800.77	956.99	892.51	1319.35	744.67
Color, habit	Yellow, prism	Yellow, needle	Yellow, prism	Orange, prism	Pale orange, piece
Crystal size, mm	0.250 × 0.160 × 0.050	0.080 × 0.030 × 0.008	0.250 × 0.150 × 0.070	0.210 × 0.120 × 0.070	0.070 × 0.040 × 0.025
Wavelength, λ	0.71073	0.74539	0.74500	0.74539	0.71073
System	Triclinic	Monoclinic	Triclinic	Triclinic	Triclinic
Space group	$P\bar{1}$	$P2_1/c$	$P\bar{1}$	$P\bar{1}$	$P\bar{1}$
Unit cell parameters					
a, Å	5.7995(5)	5.7550(12)	7.9183(14)	13.649(5)	9.411(2)
b, Å	7.4671(6)	28.948(2)	9.1314(5)	14.791(3)	9.602(2)
c, Å	18.7649(15)	12.5300(9)	11.957(3)	15.367(2)	17.726(4)
α, deg	84.147(3)	90	91.900(8)	63.878(7)	90.078(7)
β, deg	86.362(3)	97.814(15)	106.565(14)	82.554(14)	95.867(8)
γ, deg	78.466(3)	90	90.156(19)	84.220(11)	102.865(7)
V, Å^3	791.29(11)	2068.1(5)	828.2(3)	2758.6(12)	1552.9(6)
Z	1	2	1	2	2
ρ(calcd.), g/cm^3	1.680	1.537	1.790	1.588	1.593
μ, mm^{-1}	1.512	1.324	1.997	1.658	1.535
F(000)	406	980	448	1324	748
θ_{min}–θ_{max}, deg	2.184–30.543	1.872–30.225	1.864–30.993	1.555–31.029	2.176–30.629
Ranges of reflection indices	$-8 \le h \le 8$, $-10 \le k \le 10$ $-26 \le l \le 26$	$-7 \le h \le 7$, $-37 \le k \le 39$, $-15 \le l \le 16$	$-10 \le h \le 10$, $-12 \le k \le 12$, $-16 \le l \le 16$	$-18 \le h \le 18$, $-20 \le k \le 20$, $-21 \le l \le 21$	$-13 \le h \le 13$, $-13 \le k \le 13$, $-25 \le l \le 25$
Number of measured reflections	13071	25286	23795	61487	35082
Number of unique reflections (R_{int})	4828 (R_{int} = 0.0243)	5340 (R_{int} = 0.0960)	4411 (R_{int} = 0.0408)	14856 (R_{int} = 0.0654)	9551 (R_{int} = 0.0656)
Number of reflections with $I > 2\sigma(I)$	4310	3682	3783	10558	6360
Reflections/constraints/ parameters	4828/0/214	5340/0/268	4411/0/233	14856/82/715	9551/0/388
GOOF	1.094	1.018	1.060	1.031	1.010
R-factors for $I > 2\sigma(I)$	$R_1 = 0.0302$, $wR_2 = 0.0652$	$R_1 = 0.0544$, $wR_2 = 0.1347$	$R_1 = 0.0478$, $wR_2 = 0.1290$	$R_1 = 0.0504$, $wR_2 = 0.1338$	$R_1 = 0.0552$, $wR_2 = 0.1226$
R-factors for all reflections	$R_1 = 0.0369$, $wR_2 = 0.0677$	$R_1 = 0.0924$, $wR_2 = 0.1543$	$R_1 = 0.0556$, $wR_2 = 0.1352$	$R_1 = 0.0723$, $wR_2 = 0.1444$	$R_1 = 0.0956$, $wR_2 = 0.1388$
Residual electron density (min/max), e A^{-3}	–0.674/0.481	–1.326/1.308	–1.914/1.930	–1.735/1.413	–1.240/1.086

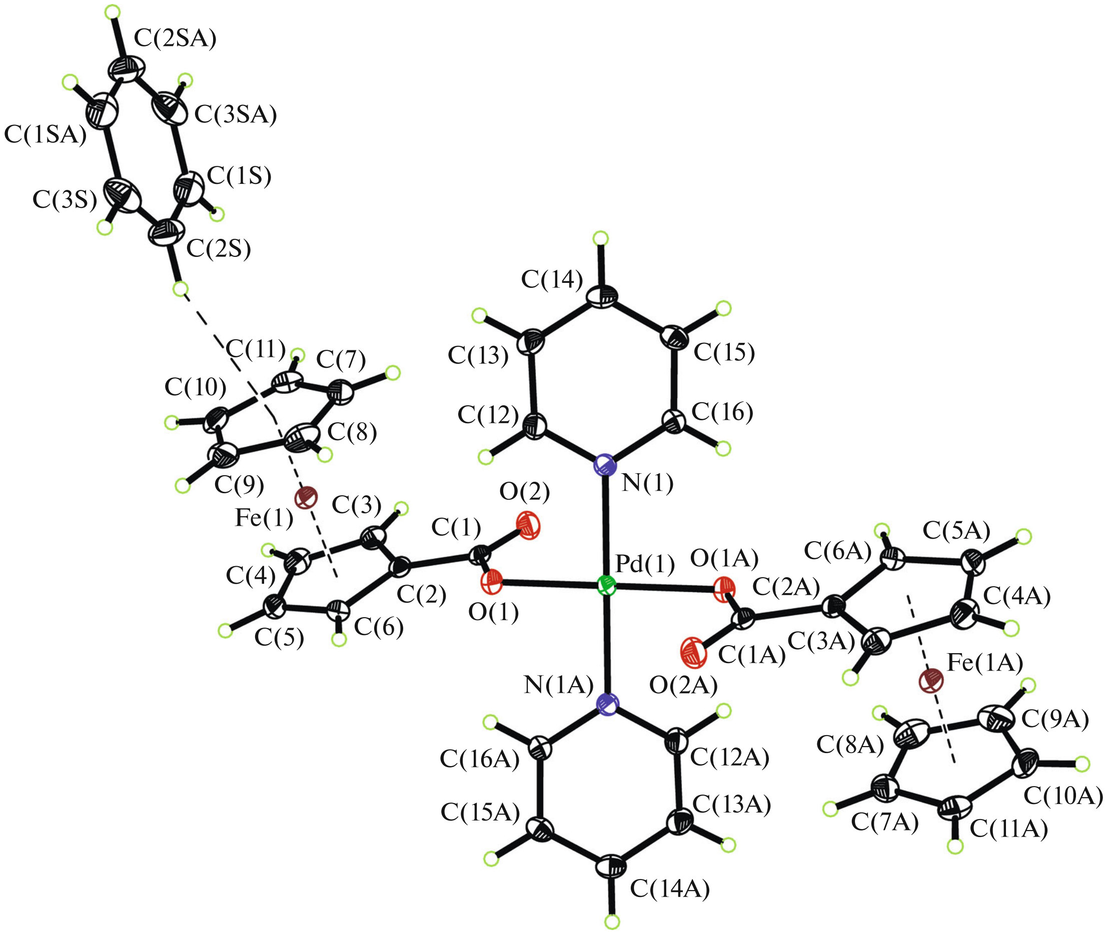

Fig. 1. Structure of the complex $[Pd(Py)_2(FcCOO)_2]\cdot C_6H_6$ (**I**). Thermal ellipsoids are drawn at 50% probability level; short C–H···π contact with hydrogen–aromatic system centroid distance of 2.786 Å is shown.

nitrogen atoms with similar interatomic distances: Pd(1)–O, 2.0056(14)–2.016(2) Å, and Pd(1)–N, 2.0355(16)–2.035(4) Å. The geometry and orientation of the rigid ferrocenecarboxylate anion do not significantly depend on the solvent, which is bound to the main molecule only by weak van der Waals forces. In all considered systems, molecules of the complex form stacks or layers, while the space between them is filled by solvent molecules of crystallization bound to molecules of the complex only by weak aromatic C–H···π contacts in the case of **I** and **II** and are easily lost (Figs. 1, 2). In the case of **III**, the solvent–complex interaction occurs via C–H···O contacts between the dichloromethane hydrogen atoms and sp^2-hybridized carboxyl oxygen atoms of the ferrocenecarboxylate anions and also via C–H···Cl contacts between the hydrogen atoms of the ferrocenyl groups and dichloromethane chlorine atoms. (Detailed information on the interatomic distances and angles in the crystals of **I**–**V** is summarized in Tables 2 and 3.)

The use of the acetate *cis*-complex with Phen, $[Pd(Phen)(OOCMe)_2]$, in the exchange reaction with the goal to prepare derivatives with the metal ratio similar to that in **I** (2Fe : 1Pd), results in the formation of crystals of mixed-metal heteroanionic complex $[Pd(Phen)(FcCOO)_2Pd(Phen)(FcCOO)(OOCMe)]$ (**IV**) (Fig. 4), in which the iron to palladium ratio is 3Fe : 2Pd. The complex is formed via strong π–π-stacking between the intermediate compound [Pd(Phen)(FcCOO)(OOCMe)] (**IVa**) (Fig. 5), in which only one of the acetate ligands of the starting complex has been replaced, and the product of complete substitution reaction $[Pd(Phen)(FcCOO)_2]$ (**IVb**) (Fig. 6). According to X-ray diffraction data, the complex crystallizes in the triclinic space group $P\bar{1}$. The two parts (**IVa** and **IVb**) can be considered as independent neutral molecules. The central palladium atom of each moiety has a square planar environment consisting of 1,10-phenanthroline nitrogen atoms (Pd(1)–N, 2.007(4)–2.008(3); Pd(2)–N, 2.014(3)–2.021(3) Å) and ferrocenecarboxylate or acetate oxygen atoms (Pd(1)–O, 1.987(3)–2.005(3); Pd(2)–O, 2.010(3)–2.014(3) Å). Analysis of the crystal packing of compound **IV** showed that molecules **IVa** and **IVb** alternate, thus forming infinite stacks arranged along

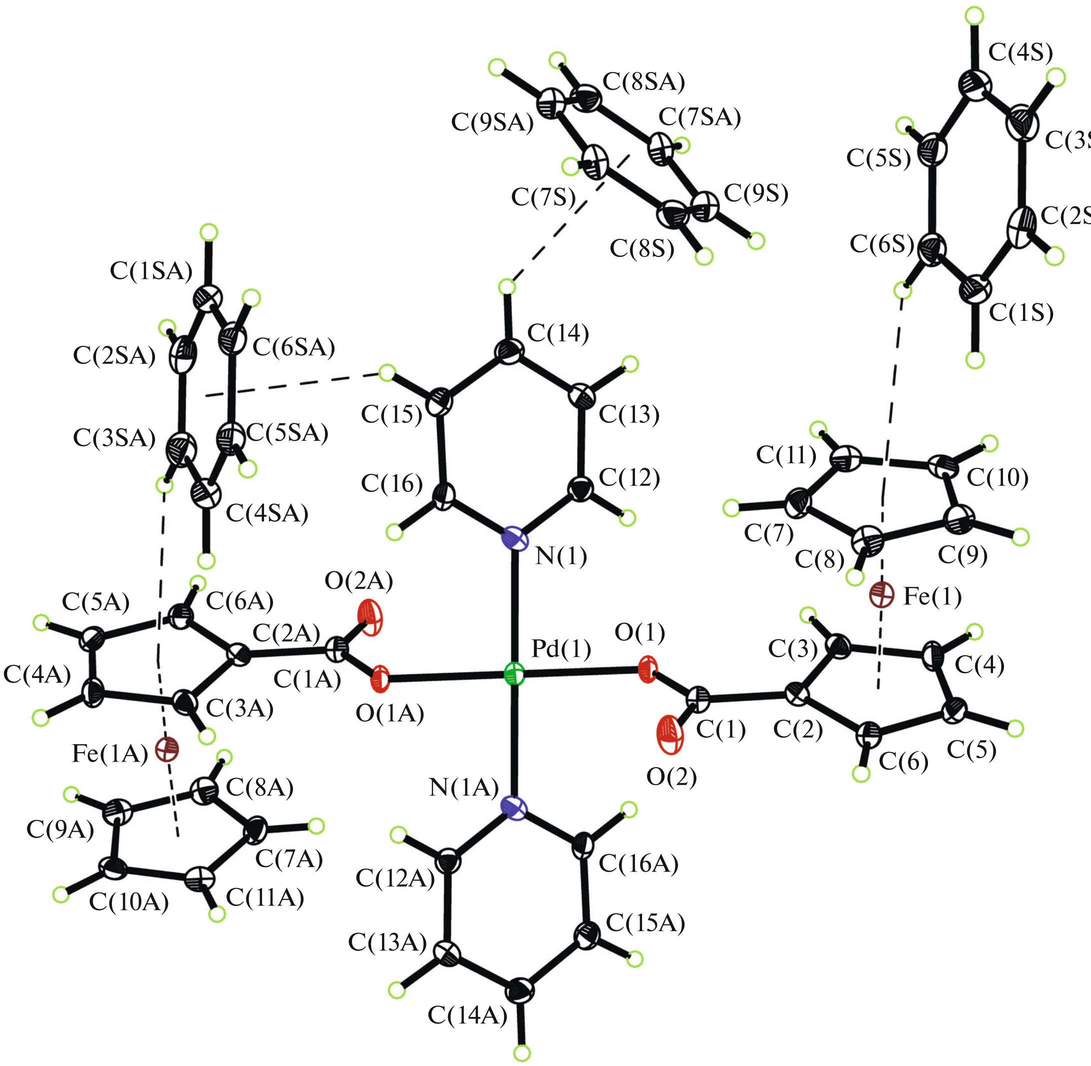

Fig. 2. Structure of the complex [Pd(Py)$_2$(FcCOO)$_2$·3C$_6$H$_6$] (**II**). Thermal ellipsoids are drawn at 35% probability level; nearest C–H···π contacts with hydrogen–aromatic system centroid distance of less than 3 Å are shown.

the *b* axis; this type of packing is due to strong π–π-stacking interaction between the aromatic systems of palladium-coordinated 1,10-phenanthrolines. It should be noted that the planes of phenanthroline ligands in the symmetrically independent part of the unit cell are somewhat non-parallel (the angle between the planes is 5.13(8)°), and the minimum distance between the main planes formed by phenanthroline and the local coordination environment of palladium is only 3.322(2) Å (within the independent part of the unit cell).

Since the previous reaction gave heteroanionic complex **IV** as the crystalline product, in order to obtain fully substituted complex [Pd(Phen)(FcCOO)$_2$] (**V**) and rule out the possible formation of side products, palladium acetate was first subjected to the replacement of acetate anions by ferrocenecarboxylate anions to give finely crystalline brown product [Pd(FcCOO)$_2$]$_n$, which was then allowed to react with Phen. Compound **V** formed in this reaction (Fig. 7) crystallizes in triclinic space group $P\bar{1}$. The key interatomic distances and angles are similar to those in **IVb** (Pd(1)–O, 1.992(3)–2.010(3); Pd(1)–N, 2.006(3)–2.017(3) Å). Like in **IV**, in this case, too, π–π-stacking interaction is detected in the crystal structure; however, the planes of phenanthroline ligands are parallel, because the crystallographically independent part of the structure contains only one molecule of the complex, and the minimum interplanar distance is somewhat greater (3.413(2) Å).

The ligand exchange reactions in palladium(II) acetate complexes resulted in the synthesis of three new heteronuclear complexes [Pd(Py)$_2$(FcCOO)$_2$], [Pd(Phen)(FcCOO)$_2$Pd(Phen)(FcCOO)(OOCMe)], and [Pd(Phen)(FcCOO)$_2$] with a high yield. The

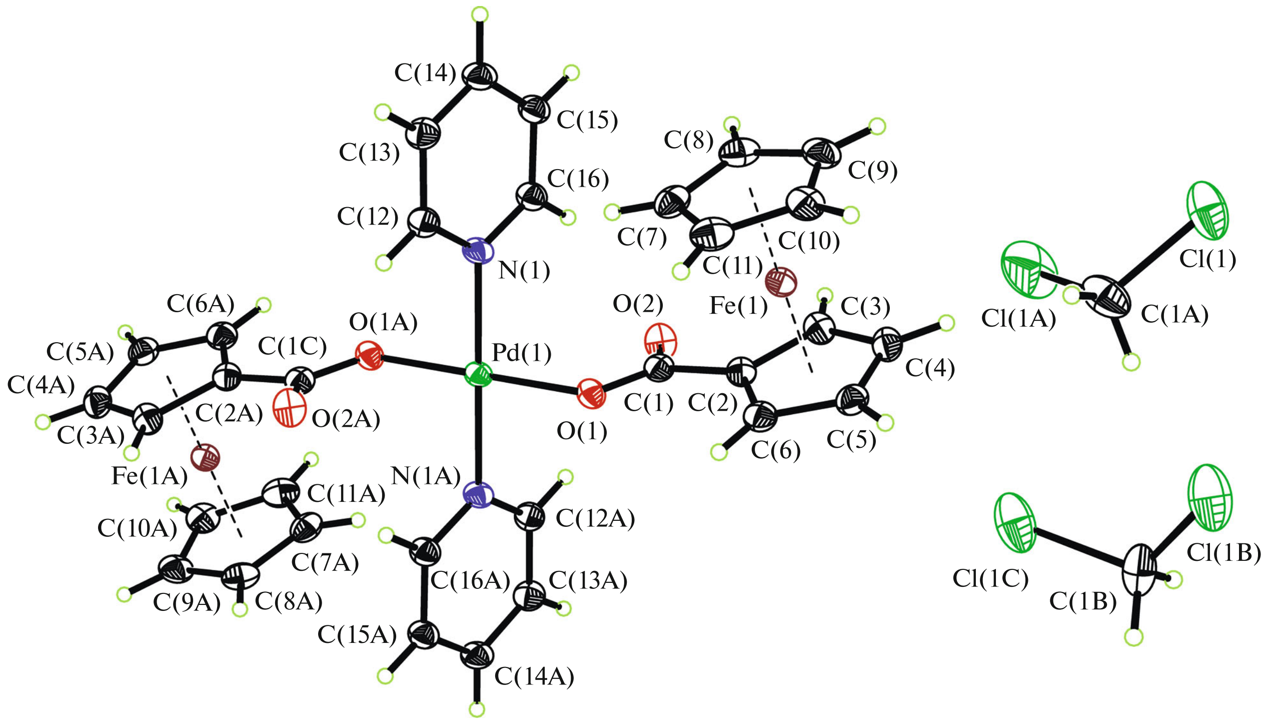

Fig. 3. Structure of the complex $[Pd(Py)_2(FcCOO)_2]\cdot 2CH_2Cl_2$ (**III**). Thermal ellipsoids are drawn at 35% probability level.

structures of these complexes in the crystalline state were established, in particular three solvatomorphs for $[Pd(Py)_2\text{-}(FcCOO)_2]$ were obtained. Ferrocenecarboxylic acid was shown to be applicable for the synthesis of palladium(II)-based bimetallic systems with different element ratios for the subsequent studies of their physicochemical properties and thermal transformations to obtain bimetallic nano-sized phases.

Table 2. Selected distances (Å) and angles (deg) in molecules **I**–**III**

Bond	**I**	**II**	**III**
		d, Å	
Pd(1)–O(1)	2.0056(14)	2.010(3)	2.016(2)
Pd(1)–O(1)$^{\#1}$	2.0057(14)	2.010(3)	2.016(2)
Pd(1)–N(1)	2.0355(16)	2.035(4)	2.016(3)
Pd(1)–N(1)$^{\#1}$	2.0355(16)	2.035(4)	2.016(3)
		Angle ω, deg	
O(1)Pd(1)O(1)$^{\#1}$	180	180	180
O(1)Pd(1)N(1)	91.04(6)	88.76(14)	89.37(10)
O(1)$^{\#1}$Pd(1)N(1)	88.96(6)	91.24(14)	90.63(10)
O(1)Pd(1)N(1)$^{\#1}$	88.96(6)	91.24(14)	90.63(10)
O(1)$^{\#1}$Pd(1)N(1)$^{\#1}$	91.04(6)	88.76(14)	89.37(10)
N(1)Pd(1)N(1)$^{\#1}$	180	180	180
Symmetry codes$^{\#1}$	$-x + 1, -y + 1, -z + 1$	$-x + 2, -y + 1, -z + 2$	$-x + 1, -y + 2, -z$

Table 3. Selected distances (Å) and angles (deg) in molecules **IV** and **V**

Bond	**IVa**	**IVb**	**V**
	d, Å		
Pd(1)–O(1)	2.010(3)	1.987(3)	1.992(3)
Pd(1)–O(3)	2.014(3)	2.005(3)	2.010(3)
Pd(1)–N(1)	2.014(3)	2.007(4)	2.017(3)
Pd(1)–N(2)	2.021(3)	2.008(3)	2.006(3)
Angle	ω, deg		
O(7)Pd(2)O(5)/O(1)Pd(1)O(3)	89.03(12)	92.53(12)	90.61(12)
O(5)Pd(2)N(4)/O(1)Pd(1)N(1)	96.80(12)	93.14(13)	95.15(13)
O(5)Pd(2)N(3)/O(3)Pd(1)N(1)	177.97(12)	173.13(12)	173.94(13)
O(7)Pd(2)N(4)/O(1)Pd(1)N(2)	172.97(13)	173.36(13)	174.54(13)
O(7)Pd(2)N(3)/O(3)Pd(1)N(2)	91.89(12)	92.45(14)	92.53(13)
N(4)Pd(2)N(3)/N(1)Pd(1)N(2)	82.15(12)	82.20(15)	81.87(14)

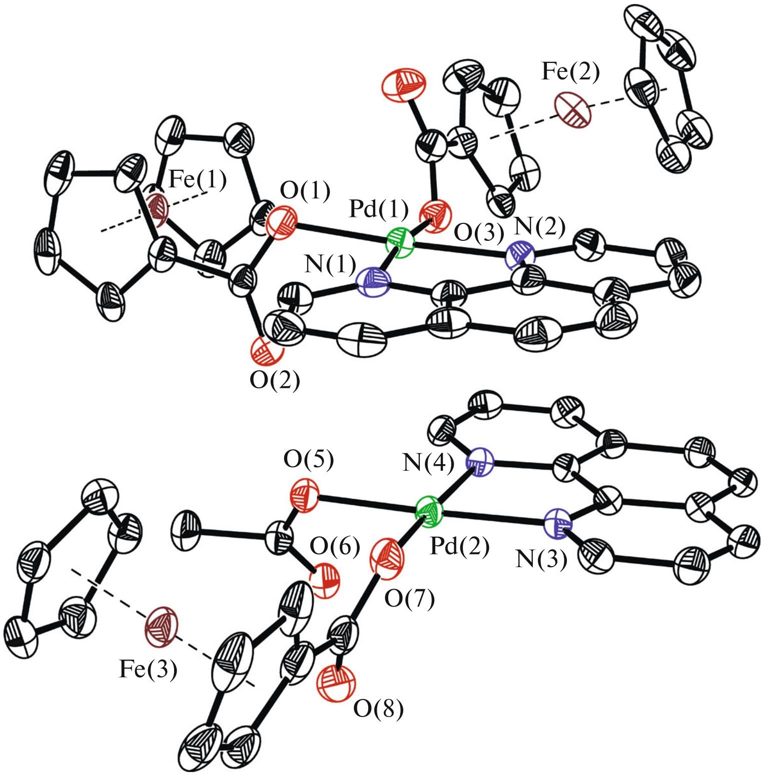

Fig. 4. Structure of co-crystallized [Pd(Phen)(FcCOO)$_2$Pd(Phen)(FcCOO)(OOCMe)] (**IV**). Thermal ellipsoids are drawn at 35% probability level. Hydrogen atoms are omitted.

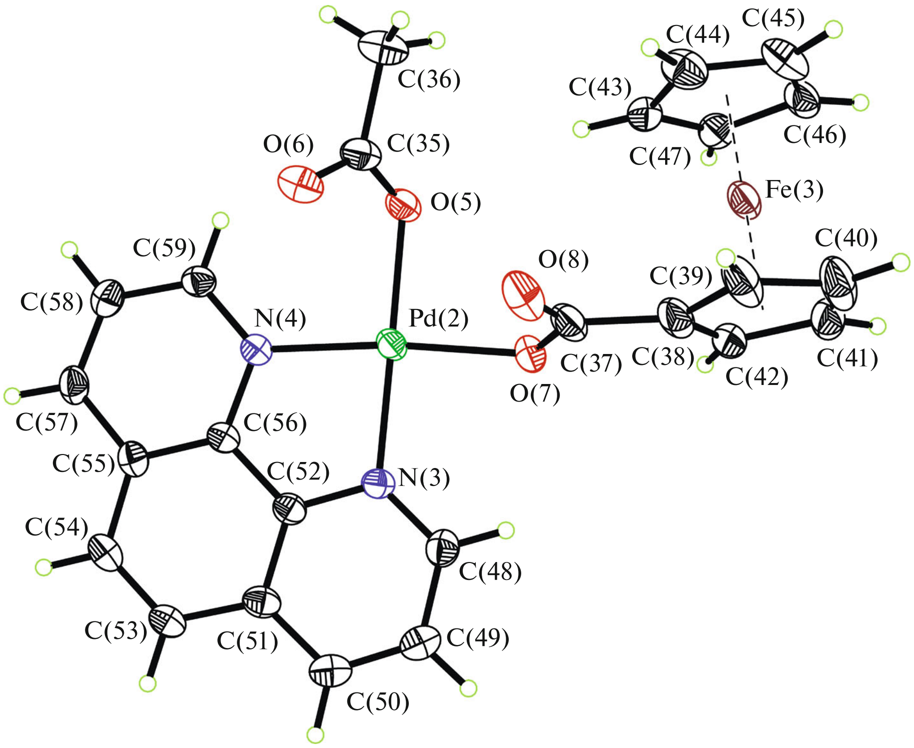

Fig. 5. Structure of the complex [Pd(Phen)(FcCOO)(OOCMe)] (**IVa**), heteroanionic moiety. Thermal ellipsoids are drawn at 35% probability level.

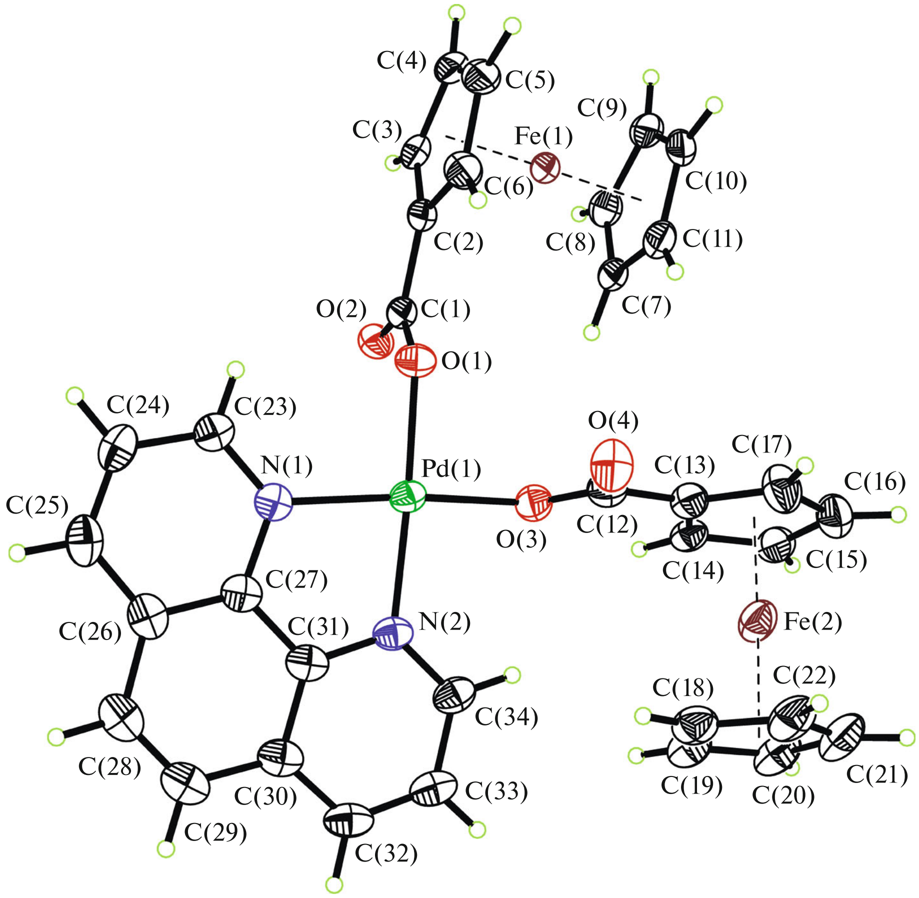

Fig. 6. Structure of the complex [Pd(Phen)$(FcCOO)_2$] (**IVb**), homoanionic moiety. Thermal ellipsoids are drawn at 35% probability level.

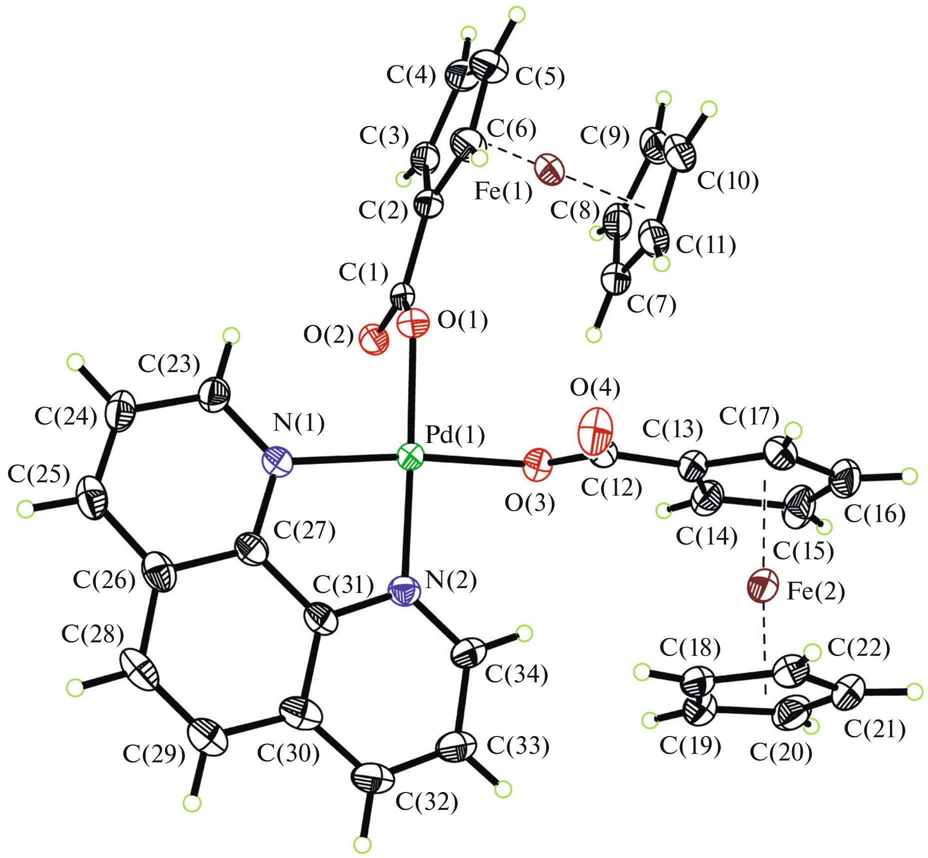

Fig. 7. Structure of the trinuclear complex [Pd(Phen)(FcCOO)$_2$] (**V**). Thermal ellipsoids are drawn at 50% probability level.

FUNDING

This study was supported by the Russian Science Foundation (project no. 18-73-10206).

CONFLICT OF INTEREST

The authors declare that they have no conflicts of interest.

REFERENCES

1. Smidt, J., Hafner, W., and Jira, R., et al., *Angew. Chem.*, 1959, vol. 71, p. 176.
2. Buchwalter, P., Rosé, J., and Braunstein, P., *Chem. Rev.*, 2015, vol. 115, p. 28.
3. Kozitsyna, N.Yu., Nefedov, S.E., Klyagina, A.P., et al., *Inorg. Chim. Acta*, 2011, vol. 370, p. 382.
4. Wang, A.L., He, X.J., Lu, X.F., et al., *Angew. Chem., Int. Ed. Engl.*, 2015, vol. 54, p. 3669.
5. Ghosh, S., Bera, S., Bysakh, S., and Bas, R.N., *ACS Appl. Mater. Interfaces*, 2017, vol. 9, p. 33775.
6. Chen, A. and Holt-Hindle, P., *Chem. Rev.*, 2010, vol. 110, p. 3767.
7. Cherkashina, N.V., Churakov, A.V., Yakushev, I.A., et al., *Russ. J. Coord. Chem.*, 2019, vol. 45, no. 4, p. 253. https://doi.org/10.1134/S107032841904002X
8. Pasynskii, A.A., Shapovalov, S.S., Skabitskii, I.V., et al., *Russ. J. Coord. Chem.*, 2016, vol. 42, p. 608. https://doi.org/10.1134/S1070328416090062
9. Kozitsyna, N.Yu., Nefedov, S.E., Dolgushin, F.M., et al., *Inorg. Chim. Acta*, 2006, vol. 359, p. 2072.
10. Kozitsyna, N.Yu., Nefedov, S.E., Yakushev, I.A., et al., *Mendeleev Commun.*, 2007, vol. 17, no. 5, p. 261.
11. Nefedov, S.E., Kozitsyna, N.Yu., Vargaftik, M.N., et al., *Polyhedron*, 2009, vol. 28, p. 172.
12. Nefedov, S.E., Kozitsyna, N.Yu., Akhmadullina, N.S., et al., *Inorg. Chem. Commun.*, 2011, vol. 14, p. 554.
13. Stolarov, I.P., Yakushev, I.A., Churakov, A.V., et al., *Inorg. Chem.*, 2018, vol. 57, p. 11482.
14. Huang, G.-H., Li, J.-M., Huang, J.-J., et al., *Chem.-Eur. J.*, 2014, vol. 20, no. 18, p. 5240.
15. Mashkovsky, I.S., Markov, P.V., Bragina, G.O., et al., *Nanomaterials*, 2018, vol. 8, p. 769.
16. Mashkovsky, I.S., Baeva, G.N., Stakheev, A.Y., et al., *Mendeleev Commun.*, 2014, vol. 24, p. 355.
17. Markov, P.V., Bragina, G.O., Rassolov, A.V., et al., *Mendeleev Commun.*, 2016, vol. 26, p. 494.
18. Stakheev, A.Y., Smirnova, N.S., Krivoruchenko, D.S., et al., *Mendeleev Commun.*, 2017, vol. 27, p. 515.
19. Smirnova, N.S., Khramov, E.V., Stolarov, I.P., et al., *Intermetallics*, 2021, vol. 132, p. 107160.
20. Grinberg, V.A., Mayorova, N.A., Pasynsky, A.A., et al., *Electrochim. Acta*, 2019, vol. 299, p. 886.

21. Yakushev, I.A., Stolarov, I.P., Cherkashina, N.V., et al., *Inorg. Chim. Acta*, 2020, vol. 508, p. 119631.
22. Mayorova, N.A., Modestov, A.D., Grinberg, V.A., et al., *Mater. Chem. Phys.*, 2021, vol. 259, p. 123968.
23. Stolarov, I.P., Cherkashina, N.V., Yakushev, I.A., et al., *Russ. J. Inorg. Chem.*, 2020, vol. 65, p. 507. https://doi.org/10.1134/S003602362004021X
24. Shapovalov, S.S., Gordienko, A.V., Pasynskii, A.A., et al., *Russ. J. Coord. Chem.*, 2011, vol. 37, p. 447. https://doi.org/10.1134/S1070328411050125
25. Pasynskii, A.A. and Shapovalov, S.S., *Russ. J. Coord. Chem.*, 2016, vol. 42, p. 574. https://doi.org/10.1134/S1070328416090050
26. Tanaka, S. and Mashima, K., Inorg. Chem., 2011, vol. 50, no. 22, p. 11384.
27. Perrin, D.D. and Armarego, W.L.F., *Purification of Laboratory Chemicals*, Oxford: Pergamon, 1988.
28. Stephenson, T.A., Morehouse, S.M., Powel, A.R., et al., *J. Chem. Soc.*, 1965, p. 3632.
29. Milani, B., Alessio, E., Mestroni, G., et al., *Dalton Trans.*, 1994, vol. 13, p. 1903.
30. *APEX3, SAINT and SADABS*, Madison: Bruker AXS Inc., 2016.
31. Svetogorov, R.D., Dorovatovskii, P.V., and Lazarenko, V.A., *Cryst. Res. Technol.*, 2020, vol. 55, p. 1900184.
32. Kabsch, W., *Acta Crystallogr., Sect. D: Biol. Crystallogr.*, 2010, vol. 66, p. 125.
33. Sheldrick, G.M., *Acta Crystallogr., Sect. A: Found. Adv.*, 2015, vol. 71, p. 3.
34. Sheldrick, G.M., *Acta Crystallogr., Sect. C: Struct. Chem.*, 2015, vol. 71, p. 3.
35. Spek, A.L., *Acta Crystallogr., Sect. C: Struct. Chem.*, 2015, vol. 71, p. 9.
36. Dolomanov, O.V., Bourhis, L.J., Gildea, R.J., et al., *J. Appl. Crystallogr.*, 2009, vol. 42, p. 339.
37. Grineva, A.A., Uvarova, M.A., Datchuk, R.R., et al., *Russ. J. Inorg. Chem.*, 2018, vol. 63, p. 610. https://doi.org/10.1134/S0036023618050091
38. Pasynskii, A.A., Shapovalov, S.S., Gordienko, A.V., et al., *Inorg. Chim. Acta*, 2012, vol. 384, p. 18.
39. Ageshina, A.A., Uvarova, M.A., and Nefedov, S.E., *Russ. J. Inorg. Chem.*, 2015, vol. 60, p. 1085. https://doi.org/10.1134/S0036023615090028
40. Shapovalov, S.S., Pasynskii, A.A., Skabitskii, I.V., et al., *Russ. J. Coord. Chem.*, 2014, vol. 40, p. 77. https://doi.org/10.1134/S1070328414020092
41. Churchill, M.R., Li, Y.J., Nalewajek, D., et al., *Inorg. Chem.*, 1985, vol. 24, no. 17, p. 2684.

Translated by Z. Svitanko